J Mater Sci (2006) 41:6751–6759
DOI 10.1007/s10853-006-0214-5

Multi-scale modeling approaches for functional nano-composite materials

Ken Reifsnider · X. Huang · G. Ju · R. Solasi

Published online: 12 August 2006

Abstract It is the general premise of this paper that multi-scale modeling with multi-physics balance and constitutive representations of the thermal, electrochemical, mechanical, and chemical phenomena that make a fuel cell work is an essential foundation for design and manufacturing. It is further claimed that such modeling enables a systems-to-science engineering approach that will accelerate technology greatly, reduce cost, improve durability, and bring fuel cell systems to life in our society. It is the objective of this paper to identify and provide a few foundation stones of understanding for such an engineering foundation for fuel cell technology, especially that part of the foundation that relates to multi-scale modeling of materials.

Multi-scale for fuel cells: the problem

We begin by attempting to identify the scope of multi-scale modeling for fuel cells that is needed to relate systems performance to the science of how the fuel cells are made and operate. As a practical matter, we want to include only those scales needed to make that connection. Figure 1 is a schematic of a generic fuel cell system.

While the heart of the system is the fuel cell itself, there is a significant balance-of-plant (BOP) configuration of tanks, pumps, and electrical equipment to complete the conversion of chemical energy into electrical power. As one would imagine, the nature of the fuel cell and the BOP is highly dependent on the application. For a cell phone, it is possible to make a micro-miniature passive fuel cell power source that is very small and has no moving parts! For an automobile, size, weight, and transient power define the design space. For factories and houses, efficiency, reliability, and durability are the primary drivers. So the first requirement is to set the specific specifications of a specific system.

To support our discussion, we select a set of specifications, outlined in Table 1; those are actual specifications for a small-scale naval device, written in general form.

As we see, not only the energy is specified (which limits range), but also voltage, weight, size, and cycles of operation are specified. As it happens, even the shape of the fuel cell system is restricted in this case. So the structural scale, in this case, fixes certain constraints on the component scale; since we are discussing fuel cells, we concentrate on those constraints, but other BOP components could be discussed as well. Two primary issues arise in the present context; fuel cell efficiency (which determines size for power and fuel requirements) is a function of operating condition, and fuel storage (which has a major effect on operability) is a function of specific power and specific energy specifications.

Figure 2 provides a foundation for discussion of the first of these issues. For fuel cells, in general, efficiency is a function of operating voltage. Fuel cell performance is usually discussed in terms of a voltage–current (or Vi) curve, sometimes called a polarization curve. Figure 2 shows a schematic of a ''typical'' response for a fuel cell. The zero current condition (open circuit condition or OCV) is fixed by the Gibbs free energy of the chemical reaction that wants to occur; if our fuels are hydrogen and oxygen that would like to form water, the available voltage associated with that reaction (in the ideal case) is 1.229 volts. If current is required of the fuel cell (in order

K. Reifsnider (✉) · X. Huang · G. Ju · R. Solasi
Connecticut Global Fuel Cell Center, University of Connecticut, Storrs, CT 06268, USA
e-mail: reifsnid@engr.uconn.edu

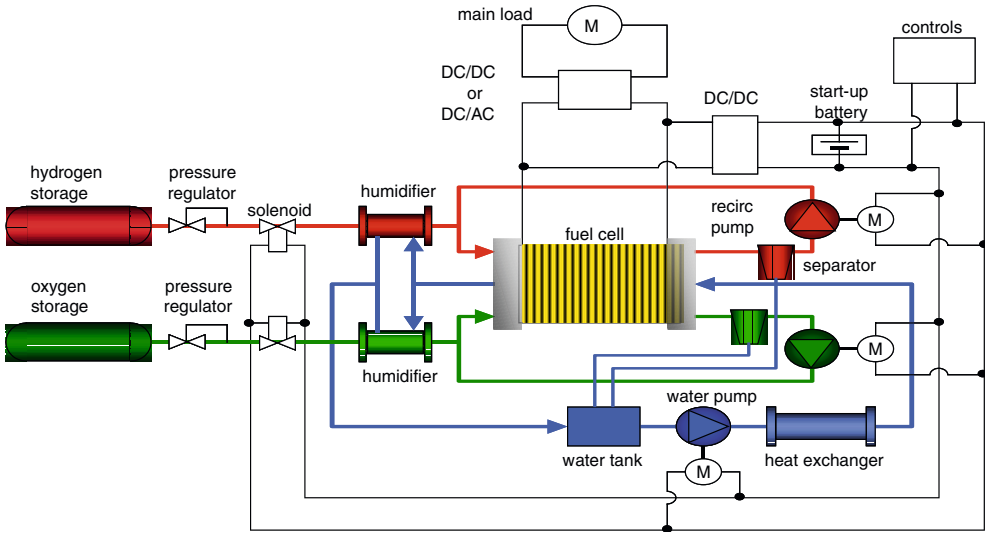

Fig. 1 Schematic of a typical fuel cell system

Table 1 Example power system requirements

Parameter	Objective
Energy	100 kW h
Bus voltage	70–90 VDC
Maximum voltage	100 VDC
Cycles	15,000
System dimensions	18″ Dia., 45″ Length
Weight	480 Lbs

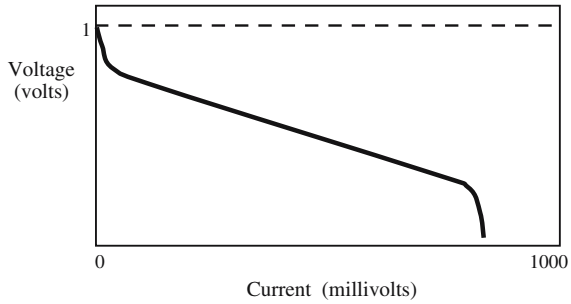

Fig. 2 Example relationship of fuel cell operating current to available voltage

to obtain power which is the product of voltage and current), then the available voltage is reduced, as sketched in Fig. 2, i.e., some power is lost to dissipative processes (or ''polarization losses''). These losses are generally associated with activation (associated with the physical limits on the speed of charge transfer), reaction ''over-voltage'' (a term used to discuss the effect of related chemical reactions that change local operating conditions, such as the effect of water production on local concentrations), concentration losses (associated with the constraints of diffusion rates in various parts of the fuel cell), and resistance losses associated with Ohmic heat production. These losses reduce the available power by the area above the performance curve in Fig. 2 and the ''ideal'' case indicated by the dotted line.

Figure 3 shows some actual data, for a solid oxide fuel cell (SOFC—we will define this cell below). In this case, the activation losses and reaction overvoltage losses, which occur at low current are small, and the Ohmic loss (defined by the slope of the mid-range) is dominant. There is very little concentration loss (dominant at high current) in this case. The power maximum, however, is at fairly high current, so one might be tempted to operate at that level (with the idea that the fuel cell size (working area and volume) can be minimized. But the Vi curves in Figs. 2 and 3 are only part of the story.

Figure 4 indicates *system* efficiency as a function of cell operating voltage. As the operating voltage drops for higher current, the system efficiency drops as well. This is clearly an engineering optimization problem, even at this point. And already we see that the problem cannot be correctly set unless the specific limits of the variables are defined by system requirements. But while we are still at the component level, let us mention fuel requirements.

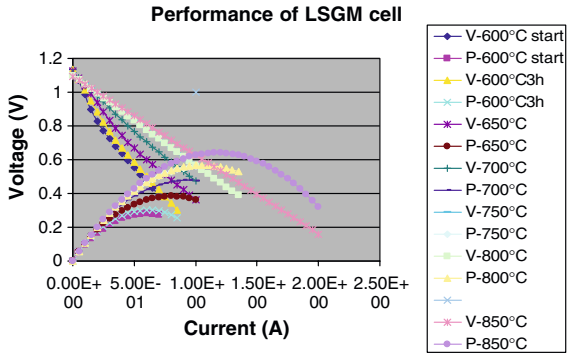

Fig. 3 Example voltage–current response of an SOFC

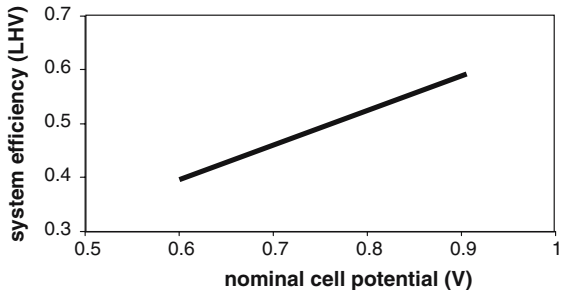

Fig. 4 System efficiency as a function of operating voltage

Like many vehicles, size and weight of the power unit is limited. In the case of our hypothetical naval device, we require a specific (small) enclosure for the power unit, and neutral buoyancy, i.e., a minimum of weight change during operation. We have many options for the fuel for a fuel cell, and many ways to carry that fuel around. (A complete discussion is off of our topic here.) But let us say that hydrogen and oxygen are the selected fuels, and that storage can be in high-pressure tanks, in liquid form, or chemical storage such as the storage of hydrogen in various hydrates. Storage as a gas takes the most space, and requires the use of some energy to compress the gas (sometimes to very high pressures). Storage in hydrates (or other materials) adds weight (sometimes a lot of weight) to the system but saves space. This is another optimization problem that is added to our design space. In some cases, the answer is a hybrid, i.e., several storage methods may be used together. In any case, the selection of fuel and fuel storage is very near the top of the list in system design. It is another reason why it is essential to go from systems to science. Now from the system scale (~10^2 m) and the component scale (~10^1 m) we pass to the materials aspects of the problem at the fuel cell/constituent (~10^{-2} m), flow/diffusion morphologies (~10^3 m), material structure/interface (~10^{-6} m), and functional material (10^{-9} m) levels.

Multi-scale, multi-physics modeling of fuel cells

Figure 5 shows two contrasting types of fuel cells in schematic form. Proton exchange membrane (PEM) cells are typically polymer based with metallic catalysts in the anode and cathode to assist in the creation of ions from fuel gases. These are low-temperature fuel cells that operate at temperatures of the order of 100 °C. Solid oxide fuel cells (SOFCs) are typically made from ceramic and high-temperature metallic parts and typically operate at temperatures of from 650 °C to 1,000 °C. Much of the Ohmic losses we spoke about earlier occur in the electrolyte layers, and is a major part of the polarization loss for SOFCs. We will discuss some of those details in a later section (at a finer scale). To minimize those (and other) losses, the electrolyte layer is generally made as thin as possible, of the order of microns. But it must prevent ''cross over'' of the gases (or liquids in other cell types) to keep the cell from ''short circuiting'' by direct conversion of the gases to water (bypassing the electrical circuit).

Most of the current literature has concentrated on the ''zoned'' models shown in Fig. 5, and two or three-dimensional versions of those models [1–3]. A recent review of such models has been presented by Faghri et al. [4]. In each zone, balance equations of mass, momentum, energy, and charge are constructed and matched at the interfaces. For this purpose, the zoned models typically divide the fuel cells into the fuel gas (hydrogen source)/fluid field, porous anode region, dense electrolyte, porous cathode, and air/oxygen flow field. Navier–Stokes and continuity equations are solved with various assumptions in

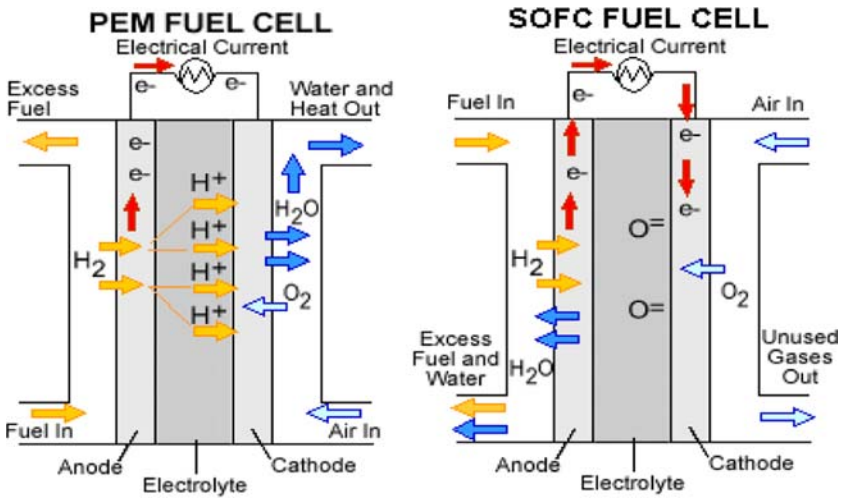

Fig. 5 Schematic diagram of the principle of operation of a PEM fuel cell (left) and SOFC fuel cell (right)

the open flow regions. However, for a PEM cell, for example, one must consider O_2, H_2O, and N_2 as separate species (when humidified air is used at the cathode) and the electrochemical reactions will change those species individually. Moreover, if any of the water vapor condenses, it may be necessary to consider two-phase flow in those regions. In the porous anode and cathode (electrode) regions, typical representations include conservation of energy and species, but since the porosity is of the order of the dimensions of the molecules being transported, Stefan–Maxwell multi-component gas diffusion is generally used. So the field equations might involve three species concentrations, temperature, molar flux, charge, and vaporization/condensation mass source as strongly coupled field variables, and a rather long list of material properties such as specific heat, conductivities, diffusion coefficients, and physical dimensions (like the surface area of liquid water).

In the catalyst regions electrochemical rate equations (e.g., Butler–Volmer forms) must be added to the mix (adding current as a field variable), and reversible as well as irreversible heat production must be included. In the electrolyte region of the PEM cell, flux of water through that region is the net effect of diffusion driven by the concentration gradient, electro-osmotic drag, and convection due to the pressure gradient across the membrane [5–7]. The flux of protons is described by the Nernst–Plank equation, which represents diffusion ions in the presence of concentration gradients and variations in local electrical fields, which interact with the charge of the ions. The material constants involve, such as the conductivities and diffusion coefficients may be functions of local hydration and temperature. Water management is a central issue in PEM cells.

By contrast, SOFC cells operate at temperatures, which preclude liquid water, and the conductivity through the electrolyte consists of oxygen (2–) ions, so in that sense the modeling is simplified. However, Ohmic resistance is a major contributor to energy loss, and activation polarization (mostly at the cathode) is a significant loss as well. This will allow us to make the transition to the next scales of consideration, the flow morphologies, material structure, and finally the nano-structure levels.

Multi-scale modeling of polarization in fuel cells

At the micron scale, the internal parts of a PEM cell might look something like Fig. 6. Carbon fiber paper might be used to diffuse the input gases, and to establish contact with the catalyst layers to provide conduction paths for the electrons that have to travel through the external circuit. Carbon (or other) particles with surface deposits of platinum (a preferred catalyst) may be bonded to the membrane with an ion-conducting polymer. The electrochemistry that drives the circuit requires that electrons be conducted to the location of oxygen reduction, that the oxygen gas be able to get there, and that the O^{2-} ions be combined with proton ions being conducted through the membrane. On the anode side, electrons must be conducted away from the oxidation site of hydrogen, the hydrogen gas must be able to get to that site, and the proton ions must have a conduction path to the membrane. (More details will be added shortly.) Hence, there is a ''triple point'' locus where ionic and electronic conduction and gas transport must coincide to enable the electrochemistry of the problem. This is inherently a geometric problem. Conduction and transport (diffusion in a porous medium) are strongly affected by geometry, and the geometry is not simply represented in a two-dimensional idealization, as Fig. 6 would suggest.

Figure 7 shows a scanning electron microcrograph of a PEM membrane-catalyst layer assembly represented by Fig. 6. The micrograph is, of course, in the plane out of the page in Fig. 6, and shows the distribution of the platinum catalyst layers and the carbon particle carriers for this fuel cell. It is clearly seen that the distribution is quite non-uniform. Indeed, we (and others) have found that the distribution is also not constant in time. Catalyst particles often migrate with time due to their unintended involvement in transport processes during fuel cell operation.

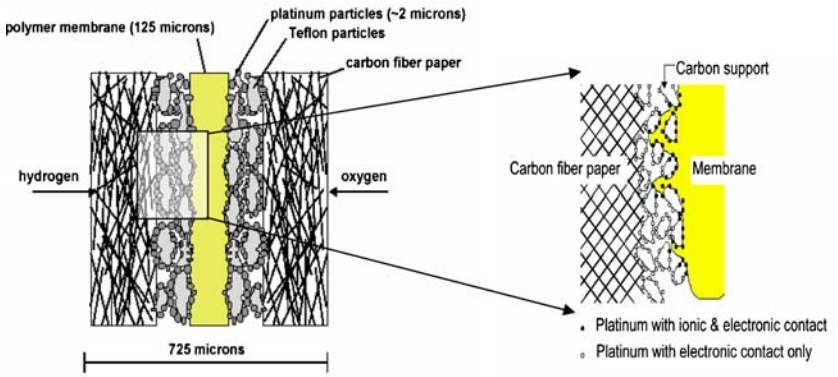

Fig. 6 Schematic diagram of a PEM cell microstructure

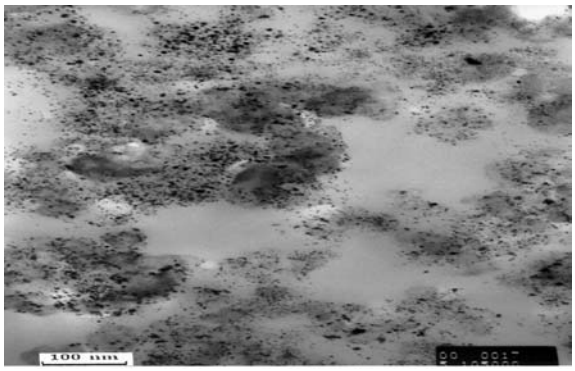

Fig. 7 Transmission electron photograph of a membrane-catalyst layer assembly

So the local geometry we just discussed is strongly three-dimensional, and not in steady state.

To bring these points together, we shift our attention to SOFC cathodes and anodes. SOFCs are typically solid state devices, that consist of ceramic electrolytes, and porous cathodes and anodes that are complex alloys that are mixed conductors. An example of such an anode is shown in Fig. 8.

Here we see that particle sizes are sub-micron, and that the ''triple point boundaries'' are at the nano-level of scale. But the properties and morphology at these scales are at the heart of the fuel cell, they control how much of the Gibbs free energy made available by the chemical reaction is available for use, i.e., how ''good or bad'' the fuel cell is. Hence, the crux of this problem is that the science of fuel cells at the nano-level is critical to it's performance (and durability) at the system level, and any truly robust design and manufacturing multi-scale analysis must consider those nano-details as part of the optimization scheme. We will select only a few examples of this point in this short discussion. Then we will close by pointing to some special needs and opportunities associated with this argument.

Effect of micro/nano-morphology and conductivity

In an earlier paper [8], we examined the effect of porosity and conductivity on fuel cell performance. The formulation

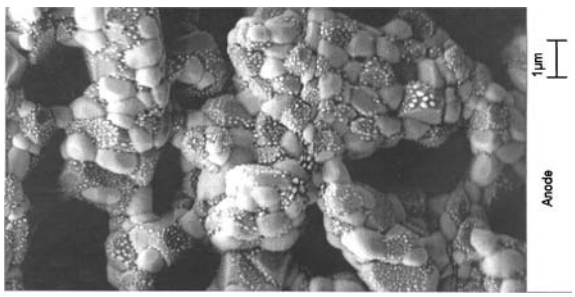

Fig. 8 SEM of an SOFC anode nano-structure

described species diffusion in the porous electrodes with Stefan–Maxwell equations, incorporating Knudsen diffusion coefficients in the porous electrodes. Knudsen diffusion coefficients can be expressed in terms of the mean pore radius and the mean free path of the gas molecules if a specific geometry of the pores is assumed [9, 10]. Chapman–Enskog theory was used to calculate the binary diffusion coefficients [11]. The conductive resistance for the mixed conductor of the fuel cell used to validate the analysis was a mixed (composite) conductor, so the Tanner/Virkar effective charge transfer resistance was used for that region [12]. A Butler–Volmer equation was used to describe the activation polarization, i.e., the energy jump before the rate-determining reaction can take place. The prediction of voltage–current response of the fuel cell (much like Fig. 3) was verified.

Then porosity in the cathode was varied in the model as one parameter study, and ionic conductivity in the electrolyte and cathode was varied for a second study. Figure 9 shows example results of that work. It should be noted, for example, that porosity in the cathode effects the charge transfer resistance of the cell in at least two ways. Gas transport is directly affected by the size and shape of the porosity, as we would expect. But more porosity also means less material available for charge transport, so there is a balance there as a function of all of the geometry, material, interface, and gas properties.

Regarding conductivity, although bulk conductivity shows little dependence on grain size (for the same volume), grain boundary conductivity is greatly affected, and that mode of conductivity is often of great importance for SOFCs.

The electrical properties of the electrolyte, for example, can be obtained by using an AC impedance measurement with an applied frequency analyzer. Guo et al. [12] studied the grain size-dependent electrical properties for YSZ electrolytes in this way. Xu et al. [13] investigated 8ScSZ and reported that although bulk conductivity is highly temperature dependent, the grain size dependency of it is not readily noticeable, however, the grain boundary conductivity shows strong dependence on the grain size, as suggested by Fig. 10. Figure 10 is a typical impedance measurement conducted at relatively low temperature to resolve the ionic conductivity contribution from both grains and grain boundaries. Taken together with an SEM micrograph, the size dependence of grain boundary conductivity can be determined.

In an effort to study the charge transfer problem with field equations to investigate this effect (instead of using one lumped bulk parameter as typically done in the literature), the representative real (observed) material microstructure was recorded for one of our samples and correct material properties were applied to analyze the local

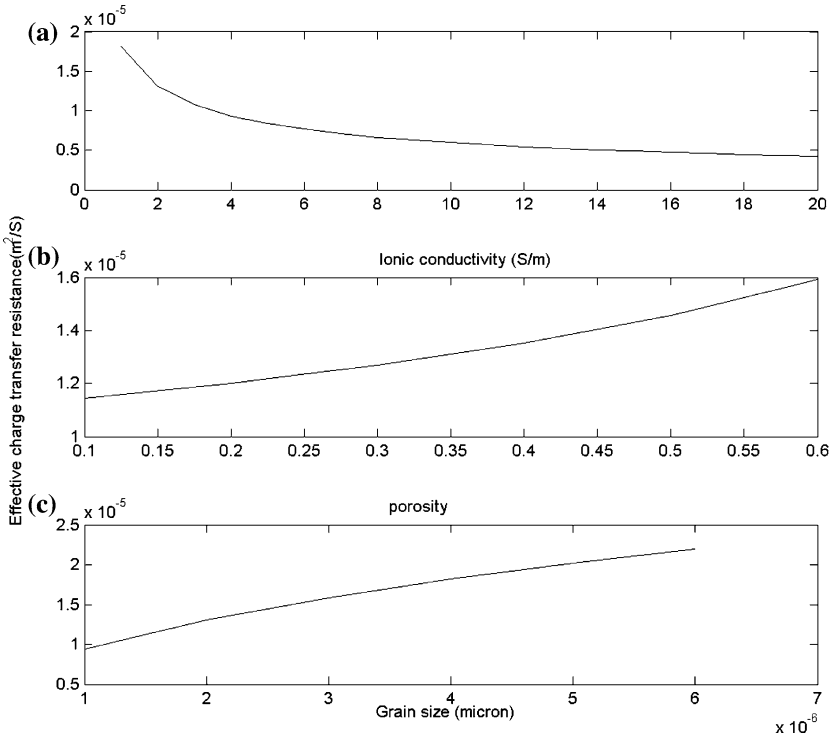

Fig. 9 Study of effect of grain size, porosity, and conductivity on effective charge transfer in an SOFC fuel cell [8]

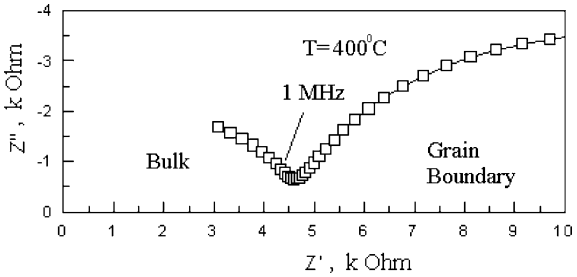

Fig. 10 Complex impedance spectra of as-sintered ScSZ at 400 °C

physics that is associated with the global properties under the assumption of charge transfer and balance.

Figure 11 shows the actual geometry observed and the finite element rendering of it used for the computations below. Based on the data of Xu [13] for 8ScSZ, the grain boundary conductivity and bulk conductivity are studied as a function of grain size and shape. The ionic (or electric) field in a conductive media is governed by the Maxwell's equation of conservation of charges:

$$\int_S \vec{J} \cdot \vec{n} \mathrm{d}S = \int_V r_c \mathrm{d}V$$

where V is the control volume with surface S, $\vec{n}$ is the outward normal to S, $\vec{J}$ is electrical current density, r_c is the internal current source (null in our case). So, applying the charge transfer described by Ohm's law,

$$\vec{J} = \vec{\sigma}^{\mathrm{E}} \cdot \vec{E} = -\vec{\sigma}^{\mathrm{E}} \cdot \frac{\partial \varphi}{\partial \vec{x}}$$

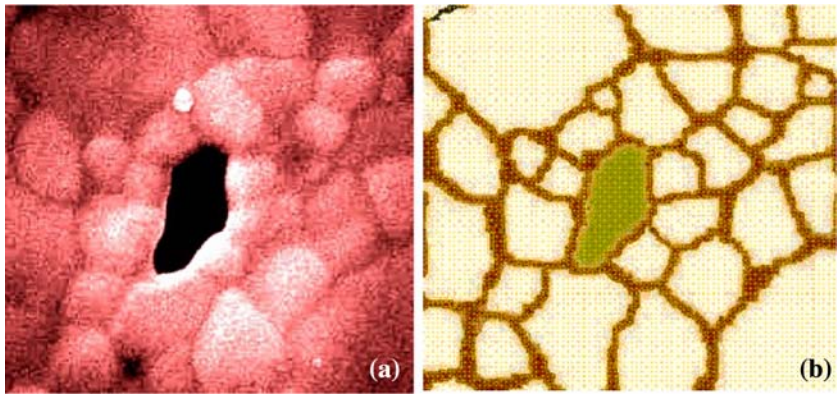

Fig. 11 Selected representative local geometry (**a**) SEM micrograph (**b**) Finite element mesh including grains and grain boundaries

where,

$\vec{E}(\vec{x})$ is defined as the negative of the gradient of the electrical potential $\vec{E}(\vec{x}) = -\frac{\partial \varphi}{\partial \vec{x}}$

ϕ is the ionic potential

$\vec{\vec{\sigma}}^{\mathrm{E}}$ is the ionic conductivity matrix.

Hence, using the divergence theorem, we can obtain the Laplace's formulation for both grain and grain boundary ionic fields, written in variational form, to illustrate the governing equation in weak form without an internal current source:

$$\int_V -\frac{\partial \varphi}{\partial \vec{x}} \cdot \vec{\sigma}^{\mathrm{G}} \cdot \frac{\partial \varphi}{\partial \vec{x}} = 0$$

$$\int_V -\frac{\partial \varphi}{\partial \vec{x}} \cdot \vec{\sigma}^{\mathrm{GB}} \cdot \frac{\partial \varphi}{\partial \vec{x}} = 0$$

where $\vec{\sigma}^{\mathrm{G}}$ stands for grain (bulk) conductivity, and $\vec{\sigma}^{\mathrm{GB}}$ is grain boundary conductivity.

For our selected representative geometry's FEM mesh the externally applied boundary conditions are as follows:

$$\mathrm{BC1} : \varphi = U1$$
$$\mathrm{BC2} : \varphi = U2$$
$$\mathrm{BC3, BC4} : \varphi \cdot \vec{n} = 0$$

Here, BC1 and BC2 are left and right boundaries; BC3 and BC4 are top and bottom boundaries (Fig. 12).

The internal boundaries between grains and grain boundaries require the following continuity equations:

$$-\vec{\sigma}^{\mathrm{G}} \cdot \frac{\partial \varphi}{\partial \vec{x}} = -\vec{\sigma}^{\mathrm{GB}} \cdot \frac{\partial \varphi}{\partial \vec{x}}$$
$$\varphi^{\mathrm{G}} = \varphi^{\mathrm{GB}}$$

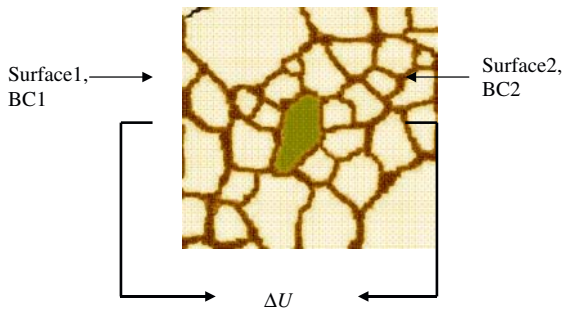

Fig. 12 Schematic of the selected local dense geometry and the applied external boundaries

The total current across the potential filed at the BC1 (or Surface1) and BC2 (or Surface2) obtained from the representative geometry is written as:

$$I_{\mathrm{Local}} = \int_{\text{Surface1, or, Surface2}} \vec{J} \cdot \vec{n}$$

Therefore, based on the charge balance, the local current is related to the global current by:

$$I_{\mathrm{Global}} = \int_S I_{\mathrm{Local}} \cdot \vec{n} \mathrm{d}S$$

Results and discussions

For $\vec{\sigma}^{\mathrm{GB}}/\vec{\sigma}^{\mathrm{G}} = 3$, the current density distribution for Surface1 and Surface2 is shown in the Fig. 13. After we integrate over the cross-section for Surface1 and Surface2, the conservation of charge is confirmed with local current $I_{\mathrm{Surface1}} = I_{\mathrm{Surface2}} = 3.842E-7(A)$.

If we increase $\vec{\sigma}^{\mathrm{GB}}$ by 20%, while keeping $\vec{\sigma}^{\mathrm{G}}$ constant at the same applied external BCs, the current density distributions are shown in Fig. 14. The integrated local total current is

$$I_{\mathrm{Surface1}} = I_{\mathrm{Surface2}} = 4.0734E-7(A),$$

which is increased by 6% compared to the first calculation.

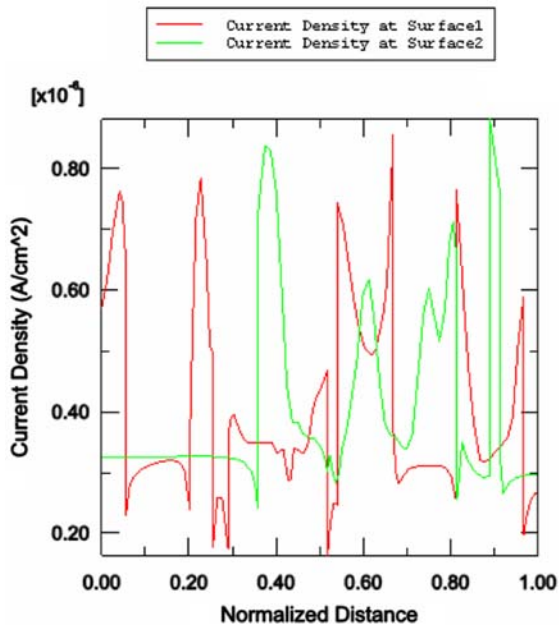

Fig. 13 Current density distribution for the Surface1 and Surface2 at $\vec{\sigma}^{\mathrm{GB}}/\vec{\sigma}^{\mathrm{G}} = 3$

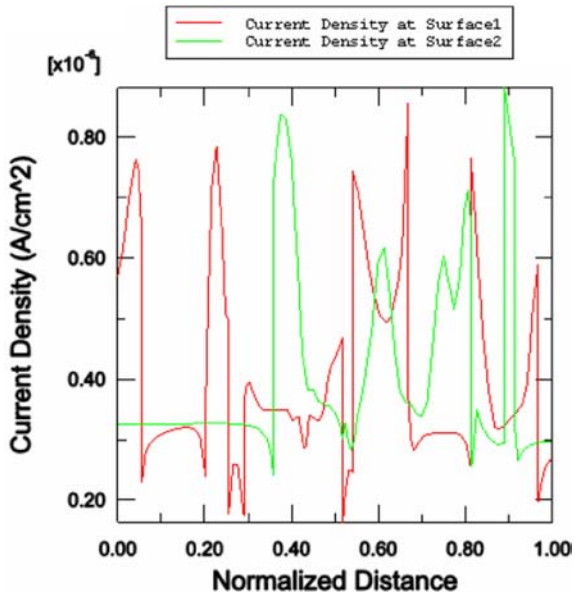

Fig. 14 Current density distribution for the Surface1 and Surface2 with $\vec{\sigma}^{GB}$ increased 20%

To study the influence on grain shape, the boundary conditions were reversed, i.e., the same potential difference was applied from left to right, and then from top to bottom for the same microstructure. The results are shown below.

The four cases studied are:

Case (1): BC2 = 0.93, BC1 = 0.9

Case (2): BC2 = 0.9, BC1 = 0.93

Case (3): BC3 = 0.9, BC4 = 0.93

Case (4): BC3 = 0.93, BC4 = 0.9.

For the Case (1) and Case (2), the total current passing through it is same (Figs. 15, 16):

$$I = 4.0734E - 07$$

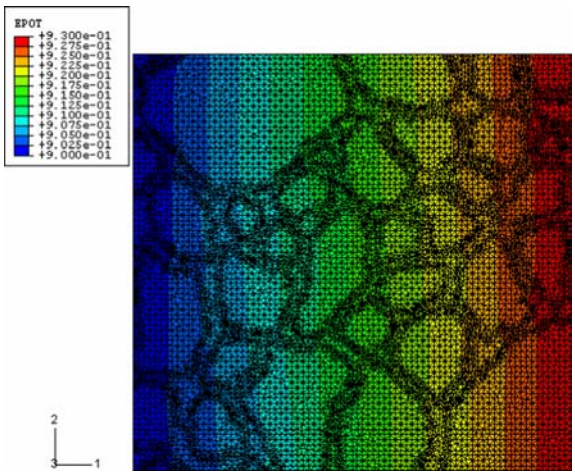

Fig. 15 Case (1)

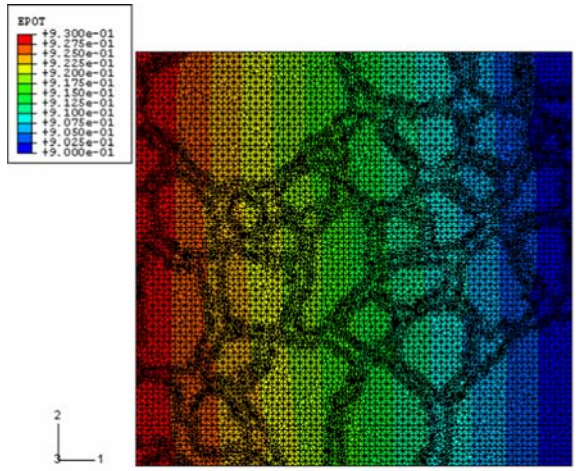

Fig. 16 Case (2)

For the Case (3) and Case (4), the total current passing through it is same (Figs. 17, 18):

$$I = 4.5919E - 07$$

From the results above, we can conclude:

1. If we reverse the boundary conditions in one direction, the total current is unchanged.
2. By comparison of Case (1)/Case (2) to Case (3)/Case (4), we can see a difference of 12.7% in total current, which illustrates that the shape of the grains and grain boundaries influence the conductivity. The computational method can determine that dependence precisely for a given microstructure, and can also form the basis for designing a microstructure for optimum results given a specific local morphology, in a cathode or anode for example.

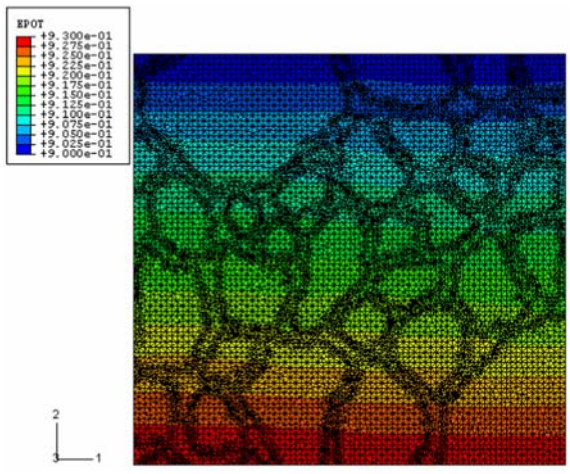

Fig. 17 Case (3)

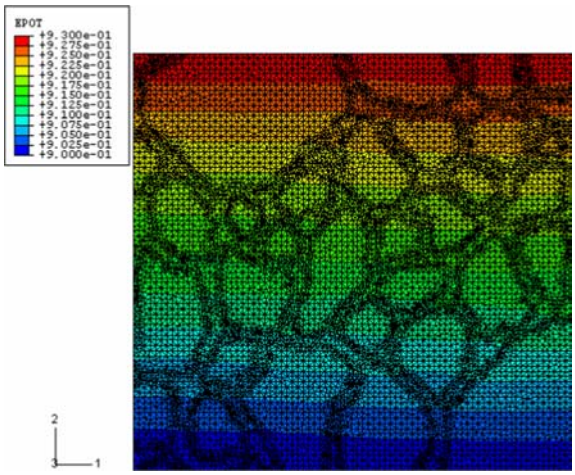

Fig. 18 Case (4)

Designing nano-structures to optimize performance

From the results that have been presented and reviewed above, it is clear that fuel cells are functional material systems that can be designed from systems to nano-structure using multi-scale, multi-physics modeling. We conclude by posing a grand challenge in this context.

The grand challenge is the concept of solving an inverse coupled multi-physics problem to specify the nano-structure of porous electrodes in fuel cells to satisfy specific system requirements for performance, i.e., to use the science of multi-physics, multi-scale modeling to design the optimized nano-structure of fuel cells based on system functional requirements (rather than material and other engineering specifications). To illustrate this idea, we consider the problem of polarization, the losses that reduce available power as output current increases (Fig. 2), as discussed above. As we discussed in Figs. 7 and 8, the nano-structure of the cathode and anode regions greatly affects the activation and diffusion-related polarization losses in a given fuel cell. Moreover, depending on the operating requirements of the fuel cell (balance of specific power, specific energy, operating voltage, burst power versus steady loads, and other variables), the optimum local nano-structure may be quite different.

Is it possible to set a multi-physics, multi-scale problem to design nano-structure for system requirements? Notwithstanding the computational power needed, it is possible in principle. There is physics and mechanics (science) missing for some parts of that problem. We do not have complete field equations, for example, to describe the function of the cathode in an SOFC. The physics steps in this process include, at least: gaseous diffusion of oxygen to the reaction sites through the porous electrodes; disassociation and adsorption of the oxygen onto the surface of the cathode material; transfer of charge to the adsorbed oxygen to create O^- ions; surface diffusion to the triple point boundary of those ions; reduction of oxygen ($O^-_{ad} + e^- \rightarrow O^{2-}_{ad}$); combining of the oxygen ion with a vacancy in the lattice of the electrolyte (YSZ in this case), so that it can be conducted to the anode [15, 16]. Each of these steps clearly involves local geometry, and if we had all of the balance equations for mass, momentum, energy, and charge, the constitutive equations, and the rate equations for the kinetics involved in place as a coupled problem, we could indeed solve this reverse engineering problem. Moreover, we could save a large fraction of the cost of the design, manufacturing, and deployment problem, and bring systems to society much more quickly.

So it is reasonable to ask, ''what *should* the nano-structure in Fig. 8 look like?'' For now, we can only say that parts of the foundation of multi-scale analysis is in place to answer that question. It is a grand challenge to provide the rest of the answer.

Acknowledgements The authors gratefully acknowledge the support of elements of this research by the US Army (DAAB07-03-3-K415), the National Science Foundation (CMS-0408807), and the Solid State Energy Alliance (DE-FC26-04NT42228). They also gratefully acknowledge the technical assistance of Peter Menard, at the Connecticut Global Fuel Cell Center, and the use of the facilities there.

References

1. Rowe A, Li X (2001) J Power Sources 102:82–96
2. Wang ZH, Wang CY, Chen KS (2001) J Power Sources 94:40–50
3. Springer TE, Zawodzinski TA, Gottesfeld S (1991) J Electrochem Soc 138:2334–2342
4. Faghri A, Guo Z (2005) Intl J Heat and Mass Transfer 48:3891–3920
5. Siegel NP, Ellis MW, Nelson DJ, and von Spakovsky MR (2003) J Power Sources 115(1):81–89
6. Zawodzinski TA, Davey J, Valerio J, Gottesfeld S (1995) J Electrochem Soc 40:297–302
7. Maharudrayya S, Jayanti S, Deshpande AP (2005) Proc FUELCELL 2005, May 23–25, Ypsilanti, MI, Paper No. 74137, ASME, 2005
8. Ju G, Reifsnider K, Huang X, Du Y (2004) J Fuel Cell Sci Technol 1:35–42
9. Sunde S (2000) J Electroceramics 5(2):153–182
10. Yakabe H, Hishinuma M (2000) J Power Sources 86:423–431
11. Neufeld PD, Janzen AR, Aziz RA (1972) J Chem Phys 57:1100
12. Tanner CW, Funf KZ, Virkar A (1997) J Electrochem Soc 144(1):21–30
13. Guo X, Zhang Z (2003) Acta Mater 51:2593
14. Xu G et al (2004) Solid State Ionics 166:391–396
15. Chan SH, Kohr KA (2001) J Power Sources 93:130–140
16. Bessler WG (2005) Solid State Ionics 176:997–1011